EXPERIMENTAL EVALUATION OF THE SCALE MODEL METHOD TO SIMULATE LUNAR VEHICLE DYNAMICS

Kyle Johnson[a], Vivake Asnani[a], Jeff Polack[a] and Mark Plant[b]

[a] NASA Glenn Research Center, 21000 Brookpark Road, Cleveland, OH 44135
[b] Youngstown State University1 University Plaza, Youngstown, OH 44503
Kyle.A.Johnson@nasa.gov, Vivake.M.Asnani@nasa.gov, Jeffrey.A.Polack@nasa.gov, Maplant@student.ysu.edu

Abstract

As compared to driving on Earth, the presence of lower gravity and uneven terrain on planetary bodies makes high speed driving difficult. In order to maintain ground contact and control, vehicles need to be designed with special attention to dynamic response. The challenge of maintaining control on the Moon was evident during high speed operations of the Lunar Roving Vehicle (LRV) on Apollo 16, as at one point all four tires were off the ground; this event has been referred to as the "Lunar Grand Prix." Ultimately, computer simulation should be used to examine these phenomena during the vehicle design process; however, experimental techniques are required for validation and the elucidation of key issues. The objectives of this study were to evaluate the methodology for developing a scale model of a lunar vehicle using similitude relationships and to test how vehicle configuration, six or eight wheel pods, and local tire compliance, soft or stiff, affect the vehicle's dynamic performance. Each wheel pod was a self-contained running gear attached to the chassis through suspension elements. The Lunar Electric Rover (LER), a human driven vehicle with a pressurized cabin, was selected as an example for which a scale model was built. The scaled vehicle was driven over an obstacle and the dynamic response was observed and then scaled to represent the full-size vehicle in lunar gravity. Loss of ground contact, in terms of vehicle travel distance with tires off the ground, was examined. As expected, local tire compliance allowed ground contact to be maintained over a greater distance. However, switching from a six-pod configuration to an eight-pod configuration, with reduced suspension stiffness, had a negative effect on ground contact. It is hypothesized that this was due to the increased number or frequency of impacts. The development and testing of this scale model provided practical lessons for future low-gravity vehicle development.

Keywords: Terrain Mobility, Moon, Scaling, Roving Vehicle, Mars, Low Gravity

1. Introduction

Roving vehicles greatly improve the efficiency of planetary surface exploration. The Lunar Roving Vehicle (LRV) was used for the last three Apollo Program missions, which allowed astronauts to traverse an order of magnitude greater distance than the first three missions (Moreo, 1988). Like off-road vehicles on Earth, the travel speeds of planetary exploration vehicles can be limited by terrain roughness. Travel over rough terrain induces vertical accelerations and at a high enough speed causes loss of ground contact.

On planetary bodies smaller than Earth, vehicles leave the ground more readily and for greater distances as the downward acceleration of gravity is relatively small. This was demonstrated on the Moon during Apollo 16 when astronauts filmed the LRV being driven at up to 10 km/hr during the so-called 'Lunar Grand Prix' (Jones, 1997). Video from this event shows the LRV pitching severely and its tires leaving the ground as it travels over terrain undulations. In the video the vehicle appears to travel in slow motion because the amount of time spent off of the ground is much more than what is expected on Earth.

Quasi-static testing of planetary rovers has become a standard practice for understanding terrain-vehicle interactions on earth (Lindemann, 2005) (Malenkov, 2016) (Meacham, Silva, & Lancaster, 2013). This type of test vehicle is constructed with the same mission weight in earth's gravity field and assumes a quasi-static interaction with soil and obstacles. Testing of this type is adequate for understanding the performance and mobility of slow speed rovers. Because of the potential severity, the dynamic motions of high-speed planetary surface vehicles must be simulated as a part of their development process. Dynamic simulation would enable vehicles to be designed with appropriate compliance to contour to the terrain at high speeds and enable low-gravity driving techniques to be developed prior to deployment. Reliable experiments are required for validation and to elucidate the phenomena that should be represented by the computer models. At this time, scale model testing according to similarity laws is the most practical experimental technique to simulate low-gravity vehicle motions on Earth. Other notional solutions, such as dynamic off-loading of each vehicle mass or accelerating the full vehicle-terrain system using an airplane, are relatively complex and costly.

The scale model method to simulate lunar vehicle dynamics depends on the ability to create a model that is dimensionally similar to the real vehicle operating in low gravity (Buckingham, 1914). As explained in (Markow, 1963), dimensional similarity between a Moon vehicle and an Earth model can be achieved using a 1/6th length scale model. At this scale, video recordings of the model's movements on Earth will appear exactly like the lunar vehicle when viewed at 6 times the original size and 1/6th the playback speed.

The challenges associated with creating and testing a 1/6th scale version of the LRV were reported by the US Army Waterways Experiment Station (WES) just after the Apollo program (Lessem, 1972). Many of the issues were associated with creating a model with 1/216th mass (mass scales with the cube of length), while transducers and electronic equipment were not readily scalable. Tire torque, rotation, and acceleration sensors were used, but the sensors and telemetry available at that time made it difficult to gather reliable data, except when driving straight. Photographic techniques were desired for vehicle motion and slip measurement, but the video technology at the time made it impractical to capture tests longer than a few seconds. Finally, they had to invest in a custom telemetry system because there were no off-the-shelf solutions for this application. Technology improvements in manufacturing, sensing, computing, and wireless communication warrant the reevaluation of the scale model method. This leads to the first objective of the present work:

1.1 Objective 1: To manufacture a scale model with a similarity relationship to a full scale lunar vehicle.

Scope and Assumptions

- The reference lunar vehicle is parameterized in Table 1. These specifications are based on the high-speed piloted lunar vehicle concept, called the Lunar Electric Rover (LER), which was being developed for NASA's Constellation program. The LER was proposed to be a pressurized module on a chassis with mobility provided by six wheel pods. Each wheel pod consisted of dual tires, propulsion and steering systems, and was attached to the chassis through active and passive suspension elements. An Earth prototype of this vehicle, created for technology development, is shown in Figure 1.
- Testing has shown that the dual tire design used on the LER is not desirable and individual tires would likely be used on future designs. Thus, the scale model will employ individual tires.
- The time and budget for manufacturing the scale model are limited to approximately 3-months and $10k, respectively, in order to help assess the practicality of using this tool for design work.
- Vehicle dynamics similarity conditions are developed by simplifying the description of the reference lunar vehicle as follows.
  - The vehicle body and wheel pods are assumed to have relatively small deformations that do not influence vehicle mobility and are therefore represented by rigid masses.
  - The suspension and tires are assumed to have relatively small inertial forces and are therefore represented by massless springs and dampers.

Grumman Aircraft Engineering Corporation also utilized 1/6th scale models, in the early 1960s to examine notional lunar vehicle configurations for the forthcoming Moon missions (Markow, 1963). From obstacle testing they determined that it was far more advantageous to reduce tire stiffness than suspension stiffness when considering impact forces and the motion response of the vehicle. This fact is only useful if tire stiffness is a free design variable; however, traction and handling requirements also affect the selection of tire stiffness.

Recently, NASA and Goodyear invented a non-pneumatic tire called the 'Spring Tire', which enables both obstacle envelopment stiffness (local stiffness) and flat ground stiffness (global stiffness) to be controlled somewhat independently (Asnani et al., 2012). The Spring Tire can be designed with low enough local stiffness to contour around an obstacle, but also have sufficient global stiffness to be responsive. The use of such a tire for driving at high speeds in low gravity motivates the second objective of this work.

1.2 *Objective 2: To implement obstacle impact testing in order to evaluate the effects of varying the local tire and suspension stiffnesses.*

Scope and Assumptions

- The test matrix is limited to the four compliance configurations shown in Table 7. The configurations being evaluated are 1) A baseline case with 6-pods and nominal suspension and tire stiffness, 2) A case with reduced tire stiffness, 3) An eight-pod configuration, where suspension stiffness has been reduced proportionally to the weight on each pod, and 4) A configuration that is the combination of cases 2 and 3. Thus, case 1 is the least compliant and case 4 is the most compliant configuration.
- The largest unavoidable obstacle height while driving on the Moon, estimated to be 15 cm, is used for impact testing. This choice was based on an educated guess considering the spatial distribution of rocks on the Moon in equatorial regions (Carrier III et al., 1991) and the state of the obstacle avoidance technology being developed for the LER at NASA Ames Research Center (Pedersen, 2009).
- It is assumed that the relative performance between compliance configurations is unaffected by suspension damping and tire-to-ground friction. Therefore, no attempt was made to scale these parameters accurately.

2. Scale model vehicle development

2.1 Reference lunar vehicle

The LER is selected as a reference lunar vehicle because it is a well-developed design intended for high-speed lunar surface travel. The Earth version of the LER (Figure 1) serves as a design reference because it is kinematically equivalent to the lunar version. According to the lunar mission architecture created for NASA's Constellation Program, the lunar version of the LER would have the features listed in Table 1 under the column 'Baseline'. Maximum travel speed was intended to be 20 km/hr, nearly twice as fast as the LRV was operated during Apollo 16's Lunar Grand Prix speed test. Thus, the vehicle's dynamic response to obstacle impacts was critical. In addition, the LER was described to have 3000 kg vehicle mass with an additional 1000 kg payload, chassis length of 4m, and tire track of 3.5m. Like the Earth prototype (Figure 1), six wheel pods would propel the LER's chassis, each with dedicated electric drive and steering systems. Each pod would also have an active suspension in series with the passive suspension, which would be used to change its relative position to the chassis and regulate the distribution of weight between tires. However, the active suspension would have a relatively low bandwidth and would not be effective in reducing impact force at high speeds (Bluethmann, et al., 2010). Thus, the passive portion of the suspension governs the vehicle's dynamic motion response at high speeds, and the active suspension was not considered for the scale model vehicle development. In addition to the baseline configuration of the LER, a notional eight-pod configuration is being evaluated. The additional pair of wheel pods serves to reduce the suspension stiffness of each pod, which is intended to make the vehicle more compliant to ground height variations. As indicated in Table 1, this notional configuration has the same total mass but would have reduced payload to account for the mass of the additional pods.

Table 1: Description of the reference lunar vehicle

Parameter	Units	Baseline	Notional configuration
Number of Pods	-	6	8
Max travel speed	km/hr	20	20
Total Mass	Kg	4000	4000
Vehicle Mass	kg	3000	3245
Payload Mass	kg	1000	755
Chassis length / Track Width	m/m	4/3.5	4/3.5

Fig 1: Earth version of the Lunar Electric Rover, created for technology development

2.2 Exact and approximate similarity

As explained in (Schuring, 1966), exact similarity can be achieved if the scale model and reference vehicle are constructed with the same materials and they are related according to the conditions shown in Table 2. With the ratio of model-to-vehicle gravity defined by G, the time ratio, T, and the length ratio, L, must be 1/G. Considering a reference vehicle in lunar gravity, G = 6, therefore T = L = 1/6. If these conditions are satisfied, the scaled motions of the model operating on Earth will represent those of the lunar vehicle.

Table 2: Vehicle dynamics similarity conditions
-The only conditions required, when identical materials and exact scaling are used.

#	Ratio	General	Lunar
1	Gravity	G	G = 6
2	Length	L=1/G	L=1/6
3	Time	T=1/G	T=1/6

Creating an exact 1/6th scale lunar vehicle, however, is unnecessarily complicated when considering only the mobility aspect of similarity. By simplifying the reference vehicle into only the elements that significantly affect mobility, the scale model may be developed with a less detailed design and using dissimilar materials. In fact, all previous efforts to create scaled lunar vehicles have implicitly used this technique (Markow, 2007) (Lessem, 1972) (Schuring, 1966). The mathematics needed to define a simplified scale model for mobility testing are detailed here.

As illustrated in Figure 2, the reference lunar vehicle is lumped into discrete sections represented by mass or compliance. Masses are used to represent sections of the vehicle where the deformations are assumed to be negligible with respect to vehicle mobility. Springs and dampers are used to represent compliant sections, where deformation is assumed to be influential but inertia is not. Accordingly, the lumped parameters equivalent system uses a single mass to represent the vehicle body and one mass for each wheel pod. Between each pod mass and the body are springs and dampers that represent the vehicle suspension and below is a network of springs that represent a tire. With this simplified representation, the Buckingham-Pi theorem (Buckingham, 1914) is employed to obtain similarity conditions that depend on the mechanical properties of each vehicle section rather than on exact design and material properties.
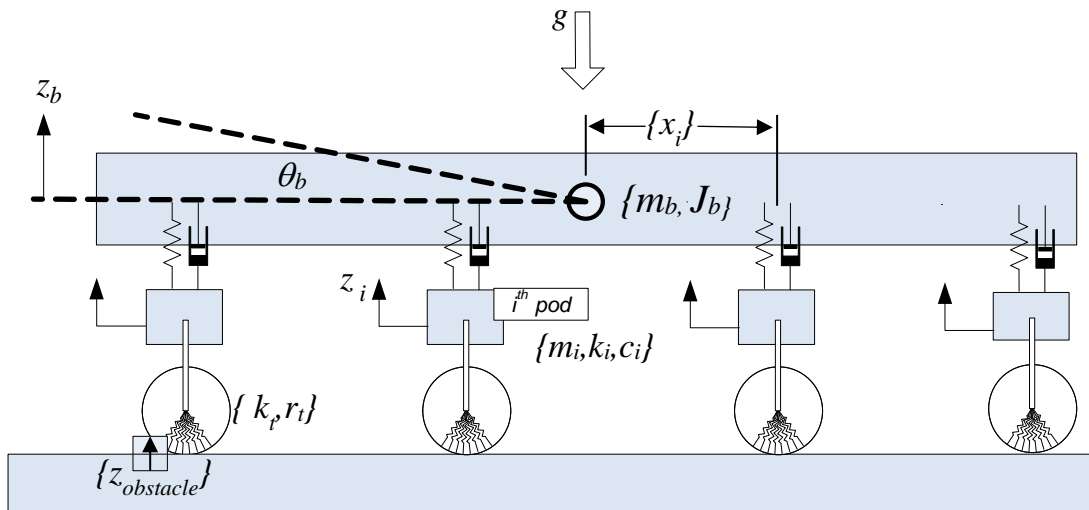

Fig 2: Schematic representation of the simplified lunar vehicle (side view)

According to Newton's second law, the governing equations of the simplified vehicle are weighted sums of the following characteristic force terms:

$$\text{gravitational force: } F_g = m \cdot g,$$

$$\text{inertial force: } F_i \propto m \frac{d^2 l}{dt^2},$$

$$\text{damping force: } F_c \propto c \frac{dl}{dt}, \text{ and}$$

$$\text{spring Force: } F_k \propto kl,$$

Where the variable definitions and associated units are listed in Table 3:

Table 3: Characteristic variables for the simplified vehicle

#	Variables	Symbol	Units
1	Mass	m	kg
2	Length	l	m
3	Time	t	s
4	Gravity	g	m/s^2
5	Stiffness	k	kg/s^2
6	Damping	c	kg/s

The variables mass, length, and time are selected to form the unit basis of the other variables. Accordingly, the equations defining the dimensionless parameters of the equivalent system are:

$$\pi_1 = g \cdot m^{\alpha_1} \cdot l^{\beta_1} \cdot t^{\gamma_1},$$

$$\pi_2 = k \cdot m^{\alpha_2} \cdot l^{\beta_2} \cdot t^{\gamma_2}, \text{ and}$$

$$\pi_3 = c \cdot m^{\alpha_3} \cdot l^{\beta_3} \cdot t^{\gamma_3},$$

where the π terms are the dimensionless parameters of a class of similar systems that can be represented by the lumped parameters model. The exponents (α, β, and γ) of these equations are solved algebraically to create the non-dimensionality, yielding the following dimensionless parameter definitions:

$$\pi_1 = \frac{g \cdot t^2}{l},$$

$$\pi_2 = \frac{k \cdot t^2}{m}, \text{ and}$$

$$\pi_3 = \frac{c \cdot t}{m}.$$

Since the scale model and the simplified lunar vehicle must have identical dimensionless parameters their terms are equated to form the following three conditions for similarity:

$$\left[\frac{g \cdot t^2}{l}\right]^m = \left[\frac{g \cdot t^2}{l}\right]^v,$$

$$\left[\frac{k \cdot t^2}{m}\right]^m = \left[\frac{k \cdot t^2}{m}\right]^v, \text{ and}$$

$$\left[\frac{c \cdot t}{m}\right]^m = \left[\frac{c \cdot t}{m}\right]^v,$$

in which superscripts m and v are used to identify the terms associated with the scale model and simplified lunar vehicle, respectively. By defining the dimensionless ratios of model parameters to those of the simplified lunar vehicle,

$$G = \frac{g^m}{g^v}, L = \frac{l^m}{l^v}, T = \frac{t^m}{t^v}, M = \frac{m^m}{m^v}, K = \frac{k^m}{k^v}, \text{ and } C = \frac{c^m}{c^v},$$

the conditions for similarity can be simplified algebraically to,

$$L = G \cdot T^2,$$
$$M = C \cdot T, \text{ and}$$
$$K = \frac{C}{T}.$$

then, by selecting $T = 1/G$, and $C = 1/G^2$, the similarity conditions for this simplified system are made to be consistent with the three conditions for exact similarity that are listed in Table 2. However, the additional three conditions listed in Table 4 are needed for the simplified representation. Using all six similarity conditions, a dimensionally similar scaled model may be developed without matching the reference lunar vehicle design or materials.

Table 4: Supplementary similarity conditions
-For dissimilar materials, and lumped representation of motion

#	Ratio	General	Lunar
4	Spring stiffness	K=1/G	K=1/6
5	Damping coefficient	$C=1/G^2$	C=1/36
6	Mass	$M=1/G^3$	M=1/216

2.3 Satisfying the similarity conditions

Gravity scaling (similarity ratio #1) is achieved naturally by testing in Earth gravity rather than lunar gravity. Time scaling (similarity ratio #3) is achieved using the experimental method explained in (Markow, 1963), whereby video of the scale model is captured and played back at $1/6^{th}$ the frame speed. The other similarity conditions are achieved by controlling the geometric and mechanical parameters of the scale model. The relevant parameters for the simplified lunar vehicle are determined based on equations of dynamic motion for a vehicle with an arbitrary number of axles, detailed in (Ingram, 1973). Considering only the bounce, pitch, and roll motions of the body and just the bounce motions of the wheel pods, the variables to be controlled are listed in Table 5. The 'Ref. value' column indicates the estimated parameters of the reference lunar vehicle (the LER). The next column, 'Scaled value', lists the target parameters of the scale model. The final column, 'Value realized', shows the parameters of the scale model that was actually created. The disparities between the values realized and scaled values will be discussed in section 3.

Table 5: Variables to be controlled
-Values are shown for the reference lunar vehicle, the scaled value, and those realized by the scale model-

Definition	Units	Ref. value		Scaled value		Value realized	
		6-pod	8-pod	6-pod	8-pod	6-pod	8-pod
Body mass (including payload)	kg	4000	4000	18.5	18.5	18.5	18.5
Pod mass	kg	122.5	122.5	0.57	0.57	0.73	0.73
Longitudinal distance body CG to the ith pod	m	-1.72, 0, 1.72, n/a	-1.72, -0.58, 0.58, 1.72	-0.287, 0, 0.287, na	-0.287, -0.097, 0.097, 0.287	-0.287, 0, 0.287, na	-0.287, -0.097, 0.097, 0.287
Vertical distance body CG to ground	m	0.85	0.85	0.142	0.142	0.168	0.154
Radius of gyration pitch, roll	m	1.04/0.95	1.02/.98	0.17/0.16	0.17/0.16	0.20/0.09	0.20/0.09
Radial tire damping	N/(m/s)	DAMPING VALUES WERE NOT CONTROLLED					
Vertical suspension damping	N/(m/s)						
Vertical suspension stiffness	kN/m	23.3	17.5	3.9	2.9	3.7	2.3
Undeflected tire radius	m	0.74	0.74	0.12	0.12	0.13	0.13
Radial tire stifness	kN/m	SEE TABLE 6 FOR TIRE STIFFNESSES					

3. Vehicle design and manufacturing

3.1 Design approach:

To begin, the CAD model used to develop the Earth version of the LER was scaled down by a factor of six. Then the parts of the design that did not relate to vehicle mobility were eliminated. This provided a small-scale vehicle design with correct kinematics and full mechanical functionality (e.g. drive, steering, suspension, etc.). Most of the subsequent effort was dedicated to modifying the design to create the mechanical properties of the scaled lunar vehicle in Table 4, and making the parts manufacturable at the small-scale.

As mentioned previously, a small-scale model with the identical materials as the reference vehicle would also have the mechanical properties that obeyed the scaling laws. However, a disproportionate amount of mass had to be removed from the structure for two reasons: 1) Electronic components tended to dominate the mass budget, once the structure was reduced to the small scale, and 2) The design of the Earth version of the LER was more massive than the lunar version would be in order to operate in Earth gravity. Alternative materials were used to reduce mass and 3D printing was used to create detailed parts that would otherwise be time consuming to create.

The design was made to be modular considering mechanical, electrical, data acquisition, and control aspects, so the vehicle could be reconfigured for this and future tests. All design decisions were made with consideration of the 3-month time frame established for creating the scale model. Finally, it should be noted, that at the beginning of the design process the similarity conditions were not well understood. As such, some of the model parameters realized were different than the intended scaled values (Table 5).

3.2 Chassis:

The scale model vehicle is depicted in Figure 3 in its eight-pod configuration. It was constructed to be strong enough to survive testing while lightweight to satisfy the scaling requirements. Additionally, it was desired that the chassis be lighter than the scaling requirements dictated so that additional masses could be added to achieve proper center of gravity and rotational inertia requirements. Honeycombed aluminum was selected as the main chassis material due to its high strength-to-weight ratio. Aluminum L brackets served as mounting points for the wheel pods and they distributed the suspension loads across the lightweight chassis. The chassis was built in four identical sections

to allow for modularity and configurability in the vehicle. Each section contained a battery, two wheel pods, and two wheel pod controllers. Depending on vehicle configuration, three or four chassis sections were attached rigidly together to form one full vehicle. The total chassis length remained constant through different vehicle configurations. In order to achieve properly scaled mass and center of gravity locations, a weight rack was added to the chassis. The weight rack ran the length of the vehicle and had several steel masses that could be added and moved to change the relative center of gravity and rotational inertia required to satisfy the scaling requirements.
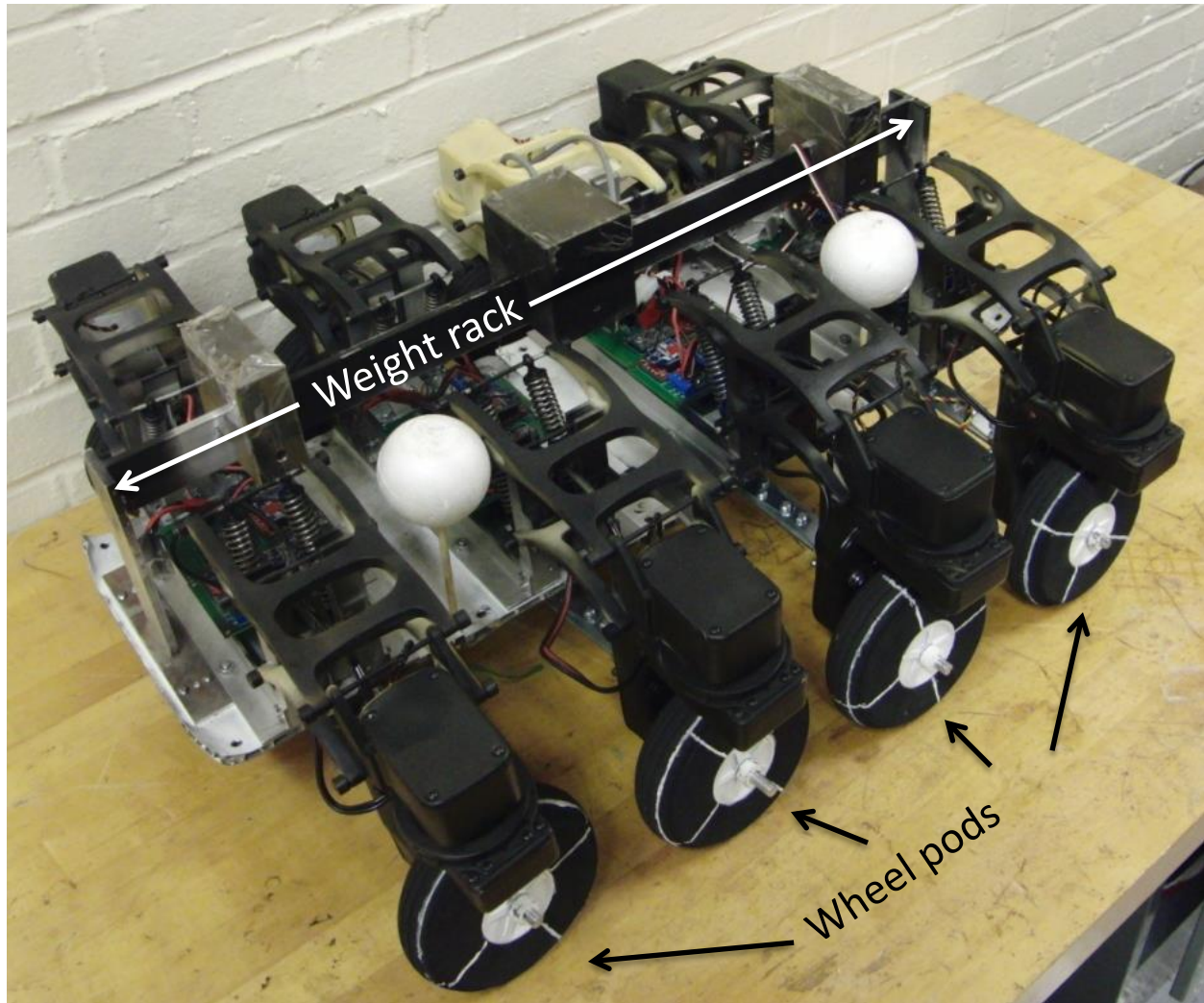

Fig 3: Scale model of the LER

3.3 Suspension:

The suspension elements for the scale model were based on the original LER design. Since machining scaled replicas of the original suspension elements was costly and impractical, 3D printed prototypes were constructed. The 3D models were adjusted to specifically take advantage of 3D printing techniques while keeping the kinematic relationships the same. The suspension arms were widened at the pivot points and the cross sectional area was increased to improve the off axis rotational strength and decrease the material stress. The suspension arms were hollowed out so that the increased size did not have a negative effect on the overall mass. DMX SL-100 was the chosen 3D printer material due to its relatively high strength-to-weight ratio (40 MPa/1.17 g/cm^3) and its availability within the time and budget constraints. The stiffness values of the 3D printed components were not measured and were assumed sufficiently rigid to satisfy the model assumptions. The springs used on the scale model were suspension elements for a small remote controlled car. Different springs were used to change the effective vertical suspension

rate of the wheel pods. The spring rates for each test configuration are listed in Table 1. The suspension appeared to be lightly damped, but damping values were not measured.

3.4 Wheel pods:

The LER is capable of steering each tire through continuous 360° of rotation. For the scale model it was determined that continuous rotation was outside of the scope, and only 180° degrees of rotation was necessary. The wheel pods were created in two parts, upper and lower. The upper part of the assembly housed a servo motor for steering and supports for the suspension arms. The lower part of the assembly was attached to the servo through a thrust bearing and housed the drive motor, encoder, and tire axle. The LER is capable of spinning each wheel pod about a point directly above the center of the drive axle and it was desired that the scale model do the same. To meet this requirement, the motor was positioned above the tire and connected by a plastic roller chain. The motors were sized such that 10 km/h travel speed was achievable. The wheel pod design went through several iterations to reduce mass, including the addition of complicated internal ribbing. The structure was 3D printed using DMX SL-100. Ultimately, the total mass of a single pod was 0.73 kg, which was 28% higher than the mass target of .57kg. This discrepancy was accepted, given the time constraints of the project.

3.5 Control system:

The control system was designed to be modular. Each wheel pod had a separate controller and shared a battery with the pod on the same chassis segment. The system was set up as a master/slave network with a single master sending signals to all the slave controllers. The slave controllers performed driving algorithms based on their pod location. Each wheel pod was equipped with a servo controller, wireless receiver, motor controller, and encoder input. The system was designed so that additional sensors could be added if desired, such as accelerometers or gyroscopes. The driving station was set up with two joysticks and a selector so that several driving modes, Ackermann, point and shoot, zero-point, and skid steer could be selected.

3.6 Tires:

One baseline tire and a tire with similar global and reduced local stiffness were selected for evaluation. The baseline tire was constructed from low density foam surrounded by rubber. The reduced local stiffness tires were constructed from foam without the rubber layer. To evaluate these designs, a common load was applied to each tire on a flat plate and then on a wedge, and the total tire deflection was measured. From this data the following stiffness metric, referred to as the 'gamma ratio', was calculated.

$$\Gamma = \frac{\delta_{plate}}{\delta_{wedge}}$$

Here δ_{plate} and δ_{wedge} are the defections of the tire on the wedge and plate, respectively. A summary of the test results is shown in Table 6. The baseline tire had a gamma ratio of 0.74, while the gamma ratio of the reduced local stiffness tire was 0.43. Damping constants were not determined.

Table 6: Summary of tire test results

Load = 30.3 N Radius = 64 mm	Baseline tire, SUL883 (Rubber)	Reduced local stiffness tire, DAVWR50 (Foam)
Flat Plate Deflection	3.56 mm 5.6% tire radius	4.06 mm 6.3% tire radius
Wedge Deflection	4.83 mm 7.5% tire radius	9.40 mm 14.7% tire radius
Global Stiffness	8500 N/m	7500 N/m
Local Stiffness	6300 N/m	3200 N/m
Gamma ratio	0.74	0.43

4. Test method

4.1 Test setup

   The test used to evaluate the scale model performance was similar to the SAE J2730 cleat test used to measure dynamic step impacts (Society of Automotive Engineers, 2006). A rectangular cleat with height 40% of the tire radius was placed in the path of the scale model. Data was collected using a high speed Phantom V10 camera. The frame was 2000 by 1200 (width by height) pixels and data was acquired at a rate of 720 images per second. The full field of view was equivalent to approximately 3 by 2 lengths of the vehicle chassis at the focal length of the camera, giving a resolution of about 0.0015 vehicle lengths. The camera was positioned 10cm above the ground so that the scale model would pass from left to right through the vertical center of the view. A 1/6th scale lunar landscape was added to the background of the test for to help create the illusion that the scale model was actually a full sized vehicle when viewing video. The cleat was located in the view so that the tire motions could be observed before and after the cleat impact. Initially the cleat was placed to impact just the right side tires. Considering that roll motions could not be observed with the camera system, the cleat was subsequently placed to create impacts on both sides of the vehicle. This

necessitated the addition of overhead rails to guide the vehicles approach angle and help to ensure the left and right tires contacted the cleat at similar time instants.
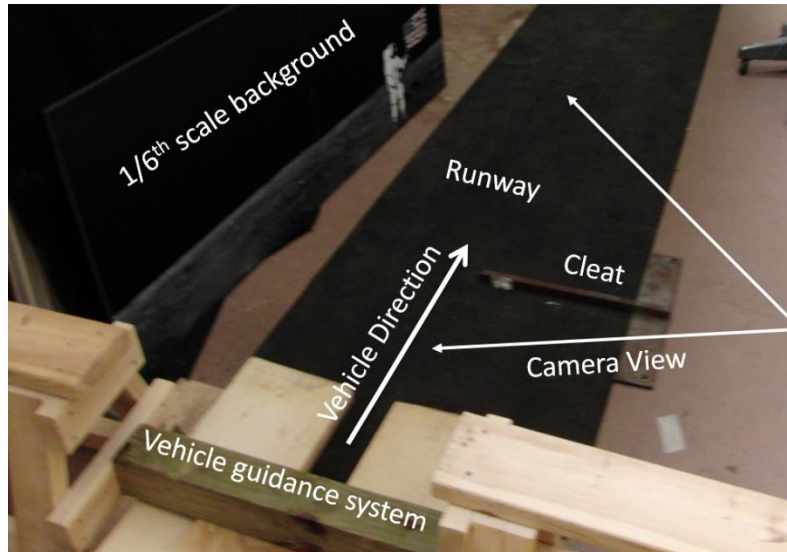

Fig 4: *Test setup*

4.2 Metrics, data processing, and analysis

The vehicle performance was assessed through analysis of the recorded images. Specifically, Spotlight-8 software was used to evaluate wheel pod translation and vehicle velocity (Klimek & Wright, 2005). Figure 5 represents one frame of the video analysis. The software tracks features by identifying contrast. To improve the reliability of this method, the vehicle was painted flat black and white radial lines were added to the tires. The centers of the tires were manually selected in preliminary images by the user and the software automatically tracked the relative displacements in subsequent images. Any increase in vertical motion after impact with the cleat was considered to be loss of contact with the ground. The horizontal distance traveled by the vehicle during loss of contact was used as a metric, since loss of contact was assumed to reduce maneuverability. It was also assumed that the vehicle reacted symmetrically, wherein the far side tires moved in the same manner as those on the near side.
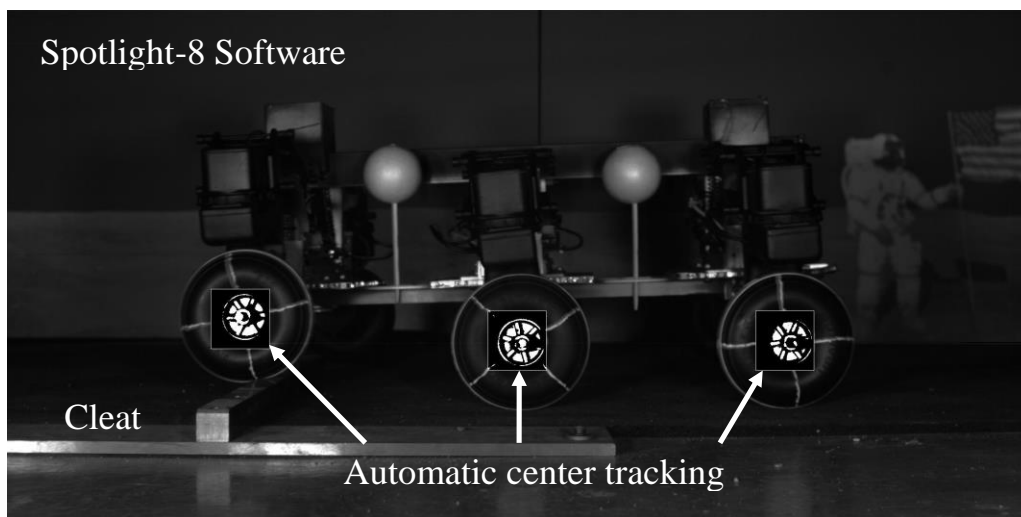

Fig 5: *Screen shot from the analysis software Spotlight-8*

5. Vehicle testing

5.1 Test configurations

Two variables were controlled for the vehicle testing, tire type (gamma ratio) and number of wheel pods. The configurations for these tests can be seen in Table 7. All testing was done at a target velocity of 10 km/h; this was the maximum speed achieved during the Apollo rover operations. In order to satisfy the scaling requirements for vehicle mass, center of gravity and rotational inertia, ballast masses were added to the weight rack. The suspension stiffness was also reduced between six and eight-pod configurations, so that the total spring rate of the vehicle was similar.

Table 7: Testing configuration matrix

#	Description	Number of pods	Suspension (kN/m)	Γ	Added mass (kg)
1	Baseline	6	3.7	0.74	6.8
2	Reduced tire stiffness	6	3.7	0.43	6.8
3	Reduced suspension stiffness	8	2.3	0.74	2.7
4	Combined 2&3	8	2.3	0.43	2.7

There were two key issues identified after the vehicle was built. The first issue was that the suspension system had more longitudinal compliance than intended. This problem was fixed by placing a third pivoting member parallel to the original suspension arms. The new joint was made of steel and provided significantly better support to the wheel pods. Unfortunately, this support eliminated the ability of the vehicle to steer and therefore a guide was built to direct the scale model's angle of approach toward the cleat. The guide was suspended above the scale model and the weight rack served as the guide follower. The second issue was that the 3D printed material, DMX SL-100, did not retain its material properties with age. Testing began a year after the initial scale model was constructed and the material softened during that time. The weight of the chassis caused the wheel pods to warp and created an inward tire camber. Due to the vehicle degradation, the amount of testing performed on the scale model was limited.

The test results for each vehicle configuration are shown in Table 8. The first column is the vehicle travel speed just prior to impact. The next three columns show the distances the vehicle traveled under conditions where tire contact was lost. As an example, the column '≥1 pair' indicates the distances the vehicle traveled with 1 or more pairs of tires off the ground. The distance data is normalized with respect to the vehicle chassis length. Each test was performed at least three times and the results were averaged.

Table 8: Test results

Configuration	Speed km/h	≥1 pair	≥2 pair	≥3 pair
		(Distance traveled normalized to chassis length)		
#1 - 6 Pod Stiff Tires	6.08	1.39	0.25	0
	5.93	1.29	0.19	0
	5.73	1.21	0.12	0
Average	**5.91**	**1.3**	**0.19**	**0**
#2 - 6 Pod Soft Tires	6.25	1.09	0.07	0
	6.01	1.05	0	0
	5.09	0.92	0	0
Average	**5.79**	**1.02**	**0.02**	**0**

#3 - 8 Pod Stiff Tires	8.18	1.78	0.63	0.13
	7.83	1.88	0.82	0.15
	7.26	2.01	0.66	0.15
Average	**7.76**	**1.89**	**0.70**	**0.14**
#4 - 8 Pod Soft Tires	5.24	1.35	0.34	0
	6.47	1.65	0.52	0
	5.87	1.53	0.48	0
	6.39	1.71	0.65	0.07
Average	**5.99**	**1.56**	**0.50**	**0.02**

6. Results and discussion

The travel speed for most of the tests was around 5.9 km/h, lower than the desired value of 10 km/h. Deterioration of the 3D printed parts made it impossible to achieve the target velocity without further damaging the vehicle. The #3 configuration was an outlier, and had speeds about 30% higher than the average. Therefore this case cannot be directly compared to the others. The 6-pod, locally soft tire configuration performed better than the locally stiff tire configuration. Specifically, for configuration 1 (6-pod and locally stiff tires), the vehicle traveled an average of 1.3 chassis lengths with at least one tire pair off the ground and 0.19 lengths with two pair off. Switching to the soft tires, configuration 2, reduced the distance traveled with 1-pair of tires off the ground by 22%. In addition, there was nearly zero distance traveled with 2 pairs of tires off the ground. The 6-pod, locally soft tire configuration also performed better than the equivalent eight-pod configuration. Specifically, configuration 2 (6-pod, locally soft) traveled about 1 vehicle length with at least 1 pair of tires off the ground and traveled near zero distance with 2 pairs off the ground. Changing to the eight-pod configuration, configuration 4, increased the distance traveled with at least 1 pair of tires off the ground by 53%. In addition, the vehicle traveled about 0.5 chassis lengths with 2 pairs of tires off the ground. This limited dataset indicates that it is preferable to use locally soft tires over locally stiff and 6 over 8 wheel pods.

It is not evident, however, that this metric of distance traveled with a specific number of tires off the ground is an adequate measure of performance. Additional testing would be required to relate tire contact to maneuverability. For instance, the additional pods could require fewer tires on the ground to maneuver adequately. It is also unclear as to why the 8-pod/low suspension stiffness configuration performed more poorly than the 6-tire configuration. Reduced suspension stiffness is generally associated with lower impact forces. However, the relatively high un-sprung mass of this vehicle type may cause high-speed impact forces to be relatively unaffected by suspension stiffness. On the other hand, the 8-pod configuration would have an increase number and frequency of impacts, which could have reduce its performance. This an unresolved issue at this point.

Compared to the US Army Waterways Experiment station (Lessem, 1972), construction and testing of a scaled lunar vehicle was significantly improved by modern technology. 3D printing technology providing an economical means to produce small and light components with detailed features to enhance rigidity. The WES vehicle used magnesium for light-weighting, which is much more expensive and difficult to work with. On the other hand the 3D printing material used for this work suffered from creep and loss of strength over time. Thus future studies of this type should select materials that are superior in this aspect. Electronics have improved significantly since the WES vehicle was built such that telemetry and sensing hardware could be substantially reduced in size and capability. This helped to meet the overall mass budge of the vehicle. However, the wheel pods were 28% more massive than the target value. This was because the electric motors mass did not scale down proportionally to length. Perhaps the most beneficial advancement from the WES experiment was the data collection and processing through photogrammetry techniques. This eliminated the need for on-board data collection hardware and provided more accurate and detailed information about the vehicle motion. The particular test setup was for 2D motion tracking of specific features on the vehicle. However, 3D motion tracking of a full vehicle is commonly done using modern tools (Creager et al., 2015).

7. Summary

The dynamic motions of planetary vehicles in low-gravity should be evaluated during early configuration studies, as this is a limiting factor for travel speed. Scale model testing is the most practical experimental method currently available. The objectives of this study were to manufacture a scale model with a similarity relationship to a full-scale lunar vehicle and to implement obstacle impact testing to evaluate alternative vehicle configurations. Exact similarity can be achieved if a scale model and vehicle are constructed with the same materials. Creating an exact 1/6th scale lunar vehicle, however, is not necessary when considering only the mobility aspect of similarity. By simplifying the reference vehicle into only the elements that affect mobility, a scale model was developed with less a detailed design and using dissimilar materials.

The Lunar Electric Rover was chosen as a reference vehicle as it was intended to travel across the lunar surface at speeds up to 20 km/h. The scale model was constructed using lightweight metal structures and detailed 3D printed parts. The objective of construction was to make the scale model easy to configure for different test objectives. The result was a modular six or eight wheel-pod vehicle that could be controlled wirelessly. Each pod was a self-contained running gear attached to the chassis through a suspension. The final scale model was close to specifications, but had higher wheel-pod mass and did not control for damping. The 3D printed material lost strength over time, which limited the vehicle testing speed and number of tests.

The test vehicle was driven over a square cleat that impacted the tires on both the left and right sides. Combinations of locally stiff or locally soft tires and six or eight wheel-pods were tested. The different types of tires were selected to represent a conventional tire and the new 'Spring Tire' design that has reduced local stiffness (Asnani, 2012). The dynamic response of the vehicle was observed and measured through photogrammetry techniques, and the distance traveled with tires off the ground was computed. Using locally soft tires had a benefit for maintaining ground contact, which was an intuitive result. The configuration with 8 wheel pods performed more poorly than that with 6 pods, and it was hypothesized that this was due to the increased number or frequency of impacts with the cleat. This work showed that the scale model method is practical for evaluating lunar vehicle dynamics and several lessons were provided to contribute to future work in this area.

List of notations

C	**Damping ratio between scaled model and reference vehicle**
c_i	Suspension damping of the ith wheel pod
F_c	Force due to damping
F_g	Force due to gravity
F_i	Force due to inertia
F_k	Force due to compliance
g	Acceleration due to gravity
G	Gravity ratio between scaled model and reference vehicle
J_b	Rotational inertia of the vehicle body
K	Spring constant ratio between scaled model and reference vehicle
k_i	Suspension stiffness of the ith wheel pod
k_t	Stiffness of the tire
L	Length ratio between scaled model and reference vehicle
M	Mass ratio between scaled model and reference vehicle
m_b	Mass of the vehicle body
m_i	Mass of the ith wheel pod
r_t	Radius of the tires
T	Time ratio between scaled model and reference vehicle
x_i	x position of the ith wheel pod
z_b	z displacement of the vehicle body
z_i	z displacement of the ith wheel pod
$z_{obstacle}$	z height of the obstacle
Γ	Gama ratio of local to global tire stiffness
δ_{plate}	Deflection of a tire when loaded against a flat plat
δ_{wedge}	Deflection of a tire when loaded against a wedge
θ_b	Rotational displacement of the vehicle body
π_1	Gravitational dimensionless parameter
π_2	Compliance dimensionless parameter
π_3	Damping dimensionless parameter

References

Asnani, V. M., Benzing, J. K., & & Kish, J. C. (2012). *Patent No. US8141606 B2*.

Bluethmann, B., Herrera, E., Hulse, A., Figuered, J., Junkin, L., Markee, M., & Ambrose, R. O. (2010). An Active Suspension System for Lunar Crew Mobility. *Aerospace Conference* (pp. 1 - 9). Big Sky, MT: IEEE.

Buckingham, E. (1914). On physically similar systems. *Physical Review Vol. IV, No. 4*, 345 - 376.

Carrier III, W. D., Olhoeft, G. R., & Mendell, W. (1991). Physical Properties of the Lunar Surface. In G. H. Heiken, D. T. Vaniman, & B. M. French, *The Lunar Source Book* (p. 529). New York: Cambridge University Press.

Creager, C., Johnson, K., Plant, M., Moreland, S., & Skonieczny, K. (2015). Push-pull locomotion for vehicle extrication. *Journal of Terramechanics, 57*, 71-80.

Ingram, W. F. (1973). *A numerical model of the ride dynamics of a vehicle using a segmented tire concept.* U.S. Army Engineer Waterways Experiment Station, TR M-73-5.

Jones, E. M. (1997). *Apollo 16 Lunar Surface Journal (Online).* NASA.

Klimek, R., & Wright, T. (2005). Spotlight-8 Software. *ver. 2005.11.23*. Cleveland, Ohio: NASA Glenn Research Center.

Lessem, A. S. (1972). Operations and Maintenance Manual for a Scale-Model Lunar Roving Vehicle. *U. S. Army Waterways Experiment Station M-72-3*.

Lindemann, R. (2005). Dynamic Testing and Simulation of the Mars Exploration Rover. *International Conference on Multibody Systems.* ASME.

Malenkov, M. (2016). Self-propelled automatic chassis of Lunokhod-1: History of creation in episodes. In *Frontiers of Mechanical Engineering.*

Markow, E. (1963). Predicted behavior of lunar vehicles with metalastic wheels. *SAE Engineering Congress & Exposition*, (p. #632J).

Markow, E. (2007). Interview with Edward Markow. NASA Glenn Research Center, Cleveland, OH.

Meacham, P., Silva, N., & Lancaster, R. (2013). The Development of the Locomotion Performance Model (LPM) for the ExoMars Rover Vehicle. *ASTRA Conference.*

Moreo, S. F. (1988). *The Second Conference on Lunar Bases and Space Activities of the 21st Century, Volume 2*, (pp. 619 - 632). Houston, Texas.

Pavlics, F. e. (2007). Interview with Ferenc Pavlics, Sam Romano, Don Freidman, and Nick DiNapoi. Santa Barbara.

Pedersen, L. (2009, September). Lunar Surface Obstacles. (V. Asnani, & J. Polack, Interviewers)

Schuring, D. (1966). Scale Model Testing of Land Vehicles in a Simulated Low Gravity Field. *Society of Automotive Engineers Automotive Engineering Congress*, (p. No. 660148). Detroit, Michigan.

Society of Automotive Engineers. (2006, August). Dynamic Cleat Test with Perpendicular and Inclined Cleats. SAE J2730.